SCIENTIFIC REPORTS

OPEN

SUBJECT AREAS:
ELECTROCHEMISTRY
BIOPHYSICAL CHEMISTRY
CHEMICAL MODIFICATION
MASS SPECTROMETRY

Received
15 February 2013

Accepted
3 May 2013

Published
21 May 2013

Correspondence and requests for materials should be addressed to I.B. (ivan.bogeski@uks.eu) or R.K. (reinhard.kappl@uks.eu)

* These authors contributed equally to this work.

Hydroxylated derivatives of dimethoxy-1,4-benzoquinone as redox switchable earth-alkaline metal ligands and radical scavengers

Rubin Gulaboski[1,3]*, Ivan Bogeski[1]*, Valentin Mirčeski[2], Stephanie Saul[1], Bastian Pasieka[1], Haleh H. Haeri[1], Marina Stefova[2], Jasmina Petreska Stanoeva[2], Saša Mitrev[3], Markus Hoth[1] & Reinhard Kappl[1]

[1]Department of Biophysics, School of Medicine, Saarland University, 66421 Homburg, Germany, [2]Institute of Chemistry, Faculty of Natural Sciences and Mathematics, ''SS Cyril and Methodius'' University, Skopje, Republic of Macedonia, [3]Faculty of Agriculture, Goce Delčev University, Štip, Republic of Macedonia.

Benzoquinones (BQ) have important functions in many biological processes. In alkaline environments, BQs can be hydroxylated at quinoid ring proton positions. Very little is known about the chemical reaction leading to these structural transformations as well as about the properties of the obtained hydroxyl benzoquinones. We analyzed the behavior of the naturally occurring 2,6-dimethoxy-1,4-benzoquinone under alkaline conditions and show that upon substitution of methoxy-groups, poly-hydroxyl-derivatives (OHBQ) are formed. The emerging compounds with one or several hydroxyl-substituents on single or fused quinone-rings exist in oxidized or reduced states and are very stable under physiological conditions. In comparison with the parent BQs, OHBQs are stronger radical scavengers and redox switchable earth-alkaline metal ligands. Considering that hydroxylated quinones appear as biosynthetic intermediates or as products of enzymatic reactions, and that BQs present in food or administered as drugs can be hydroxylated by enzymatic pathways, highlights their potential importance in biological systems.

Quinones constitute a broad class of biologically active substances (small molecules) involved in vital cellular processes such as respiration and photosynthesis[1–4]. In addition, there is also an increasing number of quinoid compounds produced mainly by plants and fungi, for which antineoplastic or antibiotic features have been described[5,6]. In the respiratory chain, the prime role of coenzymes Q is to mediate the electron transfer between various redox centers and to translocate protons across the inner mitochondrial membrane by turnover of the quinone/quinol (Q/H_2Q) redox couple. Because of these redox transitions, in cells, coenzymes Q can act as weak radical scavengers[7] and also as a source of superoxide ($^{\bullet}O_2^-$) and related oxidants[8].

For quinones in general, the structure of the quinoid core group and its substituents determines their redox-activity and chemistry which in case of the biologically and pharmacologically important benzoquinones is still not fully resolved. While the mechanistic pathway of electron transfer of quinones in organic (aprotic) media involving two successive one-electron steps seems to be unanimously defined and accepted, in aqueous solutions, quinone electrochemistry is still controversial[9–13].

It is also known that quinones readily undergo addition/substitution reactions and are structurally transformed by interacting with lipids and enzymes[14–18]. Recently, we have studied coenzymes Q (Q1 and Q10) which proved to be chemically reactive undergoing nucleophilic substitution reactions, although their quinoid ring is fully substituted with two methoxy-groups, one methyl- and an isoprenyl-group. In particular, the methoxy positions were found to be susceptible to substitution by hydroxide anions[19]. In the present study, we focus on a partially substituted benzoquinone also containing two methoxy-groups, i.e. 2,6-dimethoxy-1,4-benzoquinone (BQ), as a model for other naturally occurring benzoquinones and more complex coenzymes. The physico-chemical properties of methoxy- and dimethoxy-benzoquinones, which are found in many living organisms[15] and are part of everyday diet (for example BQ in wheat germ)[20], are strongly altered by enzymatic or chemically induced substitution or addition of hydroxyl groups[17]. Because such hydroxylation reactions are essential steps in the

biosynthesis of coenzyme Qs and other biologically relevant benzoquinones[4,15,21], this study aims to uncover mechanistic aspects of these chemical processes and to screen the emerging features of the hydroxyl-derivatives such as their redox potential, chelating properties and their pro- or antioxidant behavior particularly within biological systems.

Results

Characterization of BQ using electrochemical measurements. For a comparison of the redox properties of the parent benzoquinones with those of the quinone forms obtained in alkaline pH, we first performed cyclic voltammetry (CV) of 2,6-dimethoxy-1,4-benzoquinone (BQ) over a pH range from 1.3 to 12. The mid-peak potential ($E_{mid,p}$) of the single peak-pair attributed to a quasi-reversible electrode transformation shift about 60 mV/pH for $1.3 \leq pH \leq 8$ (Fig. 1a, b). Over the pH interval from 8 to 11, the slope is 32 mV, whereas for $pH \geq 11$ the pH dependence is lost. This behavior of the BQ/H_2BQ redox couple clearly indicates involvement of $2e^-$ and $2H^+$ for $1.3 \leq pH \leq 8$, $2e^-$ and $1H^+$ for $8 \leq pH \leq 11$ and only $2e^-$ transformations for $pH \geq 11$. These results imply that $pK_{a,1}$ and $pK_{a,2}$ of the H_2BQ acid are close to 8 and 11, which are comparable to singly or doubly alkyl-substituted 1,4-hydroquinones[22,23].

In an alkaline solution (0.1 mol/L NaOH), however, BQ exhibits a time dependent evolution of the voltammetric pattern (Fig. 1c), accompanied by a profound change of the solution color from yellow to deep red (Fig. S1a). The peak-pair I ($E_{mid,p} = -0.45$ V) of the parent BQ compound decreases gradually, while a new peak-pair (II) emerges at $E_{mid,p} = -0.65$ V, representing the electrochemical transformation of the newly formed redox active species. After 20 h reaction time, process II prevails as the reaction mixture contains mainly the final product(s). The rate of BQ transformation significantly drops at $pH < 11$ and can be completely quenched by neutralization to $pH \leq 7$. The quenched reaction mixture retains its red color and voltammetric behavior indicating chemical stability of the new product(s). At physiological pH of 7.3, the formal potential of the new process II belonging to the new BQ form(s) is 360 mV more negative compared to the process I of the parent BQ (Fig. S1b). Such negative shifts in potential were reported as a characteristic feature of α-hydroxyl benzoquinones[17] as compared to the non-hydroxylated forms indicating that the new BQ species also carry a hydroxyl-group (hydroxyl-BQ/OHBQ). The electrode process II in non-buffered aqueous solutions is pH independent over the interval $2.5 \leq pH \leq 11$, revealing significantly higher acidity of the new specie(s) (see the signal at more negative potentials in Fig. S1b). In the course of the transformation of 1 mM BQ in 0.1 M NaOH, the pH of the solution gradually drops from 13 to about 10.5 after 24 h, indicating significant consumption of OH^- anions. In addition, a series of partitioning experiments in a water/1,2-dichloroethane (DCE) biphasic system showed a higher hydrophilicity of the novel quinone products compared to the parent compound (Fig. S1c).

Characterization of BQ and OHBQ using UV-VIS spectroscopy. Because a significant change of color could be observed upon exposure of BQ to alkaline pH, we next performed UV-VIS experiments. A neutral aqueous solution of BQ has a yellow color (Fig. S1); its typical UV-VIS spectrum features two bands at 289 and 392 nm (Fig. 2a). Reduction of BQ to its quinol form using sodium borhydride ($NaBH_4$) renders the solution colorless within 4.5 min (light grey trace) reflected by the decrease of both bands. In aerated conditions, the quinol form is slowly re-oxidized, thus restoring the original BQ spectrum (Fig. 2a, see arrows and reddish traces). In an alkaline medium, two different absorption peaks at 247 and 303 nm are present, which inversely change their intensity over time (Fig. 2b). In addition, a rather broad band around 503 nm is appearing, which is responsible for the intense red color of the solution (Fig. S1). The spectral changes reveal formation of new hydroxyl BQ(s) with significantly different electronic structure compared to the parent compound, in accordance to the electrochemical behavior. Comparable pronounced bathochromic shifts were induced by the OH-substituent in α-hydroxy benzoquinones[17]. After quenching the reaction (by titration with acid) to neutral pH, the solution retains the red color, which bleaches upon reduction with $NaBH_4$ (Fig. 2c). This finding indicates that the red color is caused mainly by the new derivatives in their oxidized quinone form.

Characterization of BQ transformation using electron spin resonance (ESR) and nuclear magnetic resonance (NMR). Based on the results shown above an involvement of quinone radicals in the nucleophilic addition and substitution of benzoquinones was expected for BQ. Hence, we first performed ESR to further elucidate details of the chemical reaction between BQ and NaOH. Our results indicated that appearance of BQ-radicals is closely associated with the change in the color upon dissolving BQ in an alkaline medium. The primary radical (Fig. 3a, trace 1) is identified as the one electron reduced BQ (semiquinone) by spectral simulation comprising six equivalent protons of the methoxy groups and two quinoid ring protons (Fig. 3a, trace 2). This primary BQ-radical was described earlier[24]. However, it is gradually replaced by a second one which is relatively stable and can be observed for more than 24 h following the initiation of the reaction (Fig. 3a, traces 3 and 4 and Fig. 3b). Its spectral pattern is consistent with three methyl protons, one quinoid ring proton as modeled by spectral simulation (Fig. 3a, trace 5) and a small proton coupling exchangeable in fully deuterated solvent

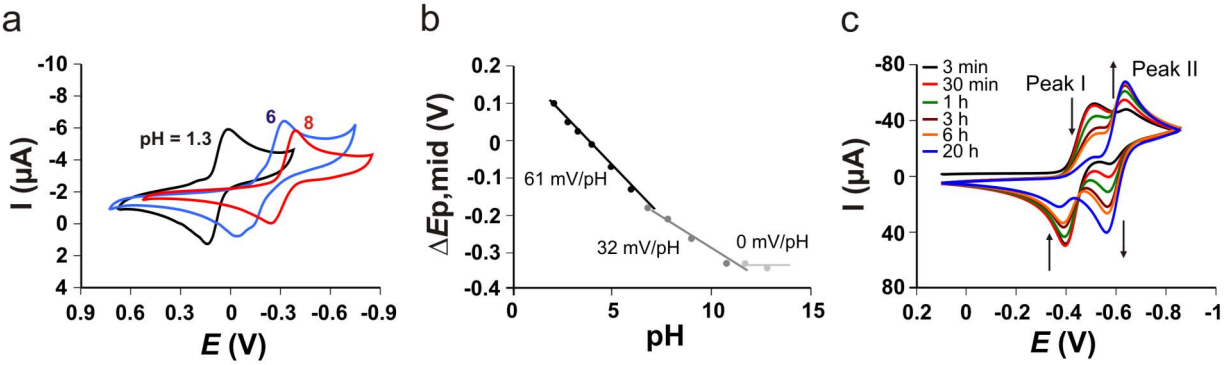

Figure 1 | Voltammetry of 2,6-dimethoxy benzoquinone. a) Cyclic voltammograms of 50 μM BQ recorded in 0.1 M buffer solutions having different pH at v = 30 mV/s. KCl-HCl solutions have been used in regions of strongly acidic pH, acetate buffers in moderately acidic pH regions and phosphate buffers in neutral and moderately alkaline pH. For pH > 10 NaOH solutions were used as electrolytes. b) pH dependence of the mid-peak potentials of CVs from a. c) Time evolution of CVs of 100 μM BQ dissolved in 0.1 M NaOH.

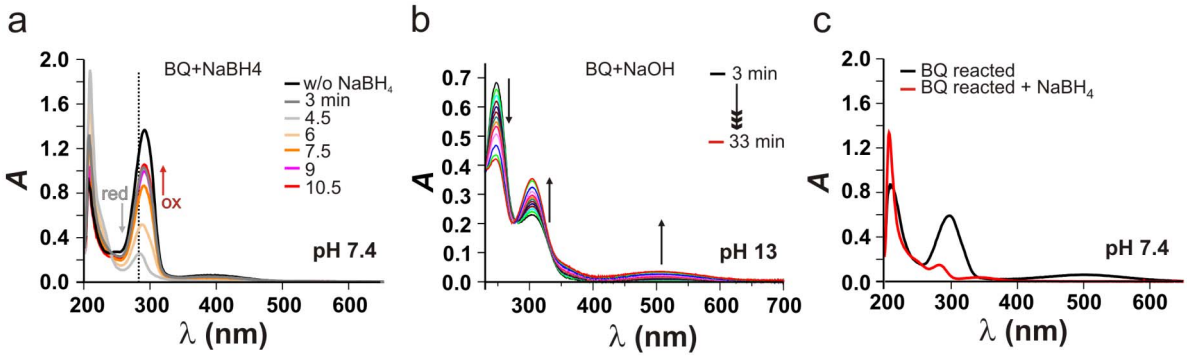

Figure 2 | **UV-VIS of 2,6-dimethoxy benzoquinone.** a) UV-VIS kinetic spectra of 10 μM BQ before (black trace) and after reduction with $NaBH_4$ (light-grey), followed by the time dependent reoxidation in air at pH 7.4. b) Kinetic spectra of 10 μM BQ in 0.1 M NaOH (pH ~13) (time increment 1.5 min). c) UV-VIS spectra of OHBQ and OHBQ reduced with $NaBH_4$ at pH 7.4.

(Fig. 3a, trace 6). This is indicative for hydroxyl substitution of one quinoid proton and one methoxy group in the parent BQ compound and formation of a new dihydroxyl, monomethoxy semiquinone derivative. The replacement of quinoid ring protons by hydroxyl-groups in non- or partially substituted 1,4-benzosemiquinones in alkaline conditions is well established[18,25,26]. However, to the best of our knowledge, substitution of other groups on the quinoid ring with a hydroxyl group was never reported in the past.

According to our results, one hydroxyl group of the secondary radical must have very high pKa value due to the presence of the exchangeable proton at pH 13. The kinetics, particularly of the second radical, for which the curve in Fig. 3b suggests a sequential

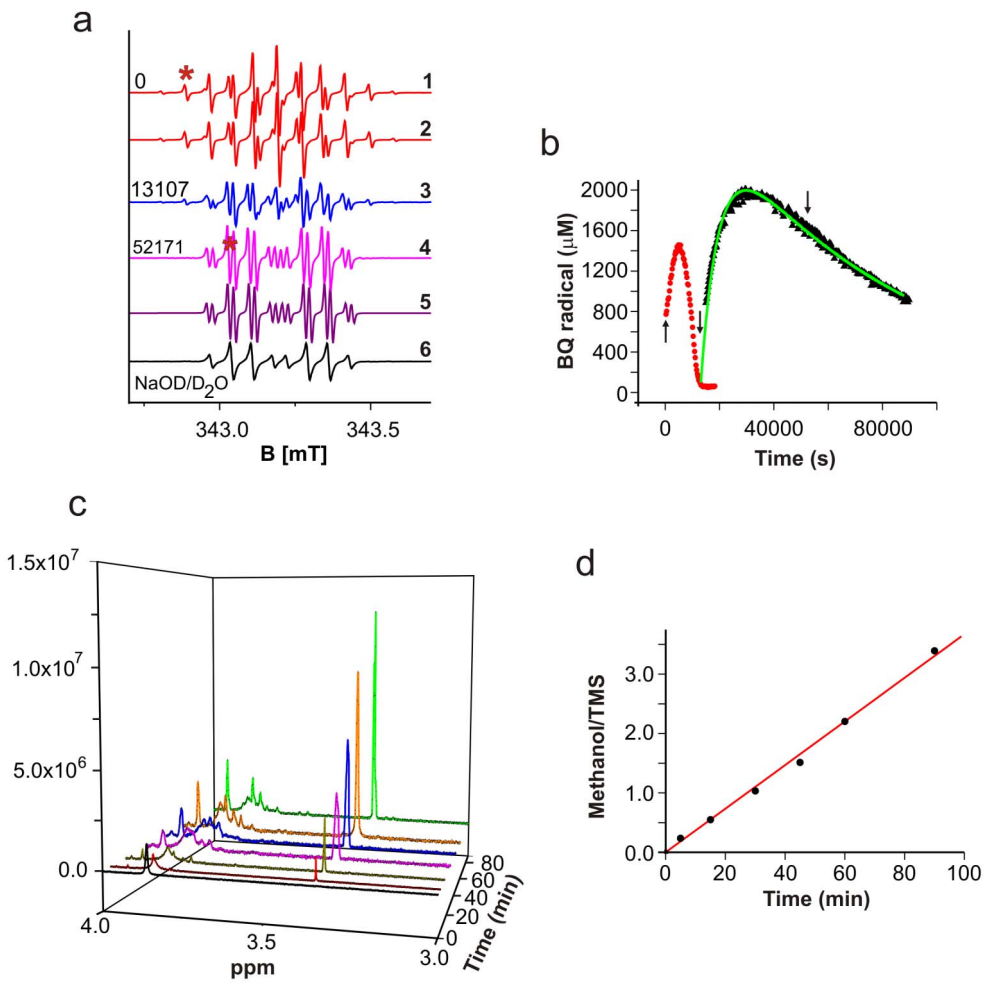

Figure 3 | **Structural transformations of 2,6-dimethoxy benzoquinone in alkaline pH observed by EPR and NMR.** a) EPR spectra of 5 mM BQ in 0.1 M NaOH (NaOD) at times (in s) indicated and spectral simulations. Asterisks mark lines used for quantitative evaluation in b. b) Evolution of primary and secondary radical, arrows indicate the corresponding spectra in a, the green curve is a fit with sequential reaction model. c) NMR spectra in the methanol and methoxy proton region of 1 mg/mL BQ reacted in 0.1 M NaOD for different times, and re-titrated to pD ~7 with DNO3. d) Ratio of the relative integrals from the signal of methanol and TMS.

Table 1 | Identification of BQ and its four most prominent hydroxyl derivatives by HPLC/DAD/MSn

Comp. No	t_R (min)	λ_{max} (nm)	$[M+H]^+$	MS^2	MS^3
1	4.5	250	189	171, 153, **143**, 127, 115	**115**, 87
2	20.9	284	185	167, **157**, 139, 125	**143**, 125, 115
3	27.2	290	169	**141**, 127, 109	**127**, 113, 109
4	29.6	294	307	**237**	223
5	37.3	294	321	**307**	**291**, 279, 263, 235

reaction, is very slow. If the solution is neutralized at any time of the reaction, the radicals are lost but the red color is preserved (see above).

The quenching of radicals upon neutralization allows performing NMR experiments. For native BQ, the peaks of quinoid protons at 6 ppm (not shown) and of methoxy protons at 3.86 ppm (Fig. 3c) are visible in a 3 : 1 ratio, as expected. For reacted and neutralized solutions, we observed drastic spectral changes in the region of the methoxy protons and a new signal at 3.36 ppm, typical for methanol (Fig. 3c). The latter increases linearly with reaction time (Fig. 3d), strongly suggesting a substitution mechanism of at least one methoxy group in BQ. Besides the formation of the complex pattern in the methoxy peak region, additional new lines are found around 4.4 ppm and in the range between 5.5 and 6 ppm (not shown).

High-performance liquid chromatography and mass spectrometry (HPLC/MS). The observation of quinone radicals in ESR and the indications of the presence of novel hydroxyl benzoquinone species from the electrochemical, spectroscopic and NMR experiments led us to perform tandem HPLC/DAD/MS experiments and identify their molecular structure. The complexity of the chemical reaction depends on the reaction time and concentration of both BQ and hydroxide ions. A typical set of HPLC/DAD/MS data is given in Table 1, while the corresponding molecular structures are sketched in Fig. 4. The data refer to a chemical reaction between 100 μM BQ and 0.1 M NaOH, which was quenched by neutralization to pH 7 after 120 min. Besides the parent BQ (compound 3), four major hydroxylated derivatives (OHBQ) are detected, present either in a quinol form (1) (λ_{max} = 250 nm) or in a quinone form (2, 4, and 5 with λ_{max} ≈290 nm, Table 1 and Fig. 4). As can be inferred from the structure of compound 2, ring protons of the parent BQ compound are prone to nucleophilic substitution with OH^-. More importantly, the structure of the other four compounds clearly shows that at least one methoxy group in the parent BQ is substituted with a hydroxyl group as already indicated by ESR and NMR data. The structure of OHBQs 4 and 5 shows that in a neutral medium, poly-hydroxyl derivatives stabilize in condensation reactions yielding dimeric compounds. The assumed molecular structures of the initial monomeric molecules are given in Fig. 4. The structure of the monomer 4 M′ agrees completely with the structure of the second radical detected by ESR. This compound, together with its semiquinone radical form, seems to be stable only in a basic medium, while undergoing condensation reaction in a neutral medium. The radical derived from dimer 4 can give the same ESR pattern as the radical of 4 M′, provided that the spin delocalization in both radical species is similar. Compounds 1 and 5 M″ are quinol and quinone forms of the same compound (2,3,5-trihydroxy-6-methoxy-1,4-benzoquinone), respectively. Obviously, the quinol form 1 is quite stable in a neutral medium. The reaction pathways (see below), include an OH^- nucleophilic Michael addition

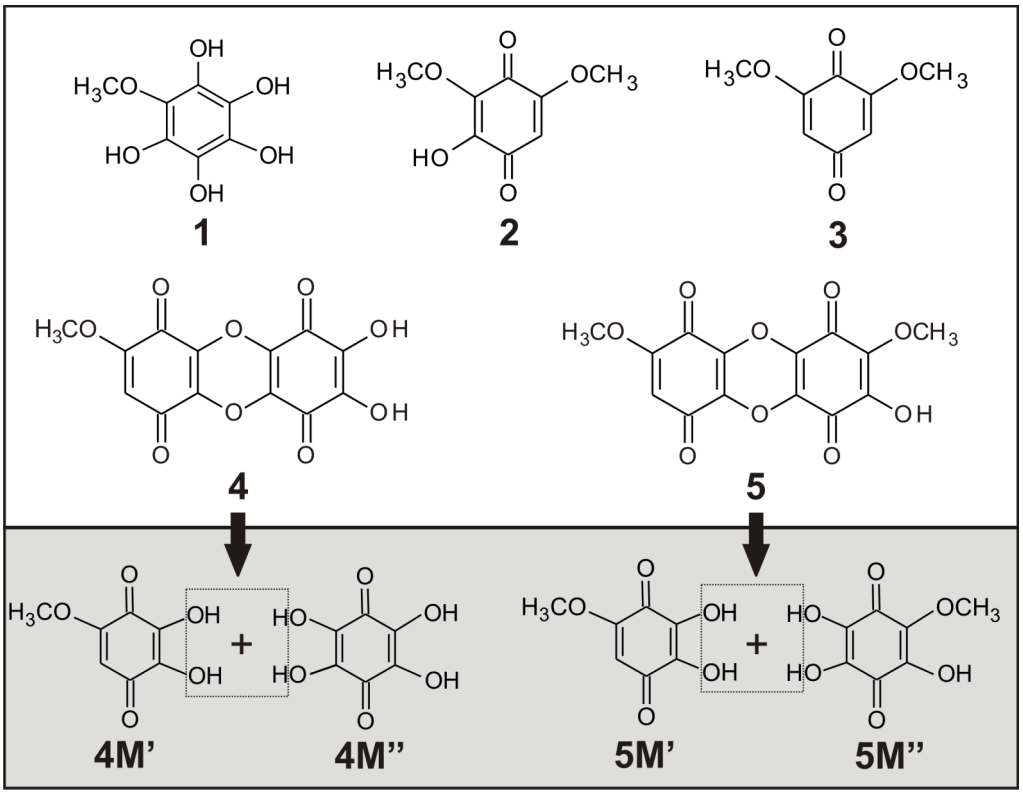

Figure 4 | Molecular structures of native BQ (3) and the OHBQ derivatives obtained by its reaction with 0.1 M NaOH.

reaction at the free positions of the quinone ring to yield quinol derivatives, or nucleophilic substitution reaction of methoxy group to yield quinone derivatives.

Properties of the novel hydroxyl benzoquinones. *Ligands of earth-alkaline metal ions*. Having identified the structures of the major hydroxylated BQs, we next analyzed their redox and chemical properties. Based on the previous findings that quinones can actively be involved in the homeostasis of Ca^{2+} in biological systems[19,27,28] the question arose whether the newly obtained OHBQs also possess similar properties. To answer this question we first tested the sensitivity of the OHBQs for earth-alkaline metal cations with voltammetry. These experiments revealed a profound sensitivity of the OHBQs to the earth-alkaline metal cations (Ca^{2+}, Ba^{2+} and to a much lesser extent to Mg^{2+}), while being insensitive to alkali metal cations (K^+, Na^+, Cs^+, Rb^+) and NH_4^+. The square-wave (SW) voltammetric response of OHBQs (peak II, Fig. 5a) shifts consistently in a positive potential direction by increasing the concentration of the earth-alkaline metal cation, the effect increasing in the order $Mg^{2+} < Ba^{2+} < Ca^{2+}$ (Fig. 5 and Fig. S2). The SW peak potential shifts linearly with the logarithm of the cation concentration, with almost Nernstian slope ranging from 55 to 62 mV (Fig. 5b). This shift reveals a redox switching complexation mechanism, in which the electrochemically reduced (quinol) form of OHBQs is able to complex these cations. In addition, the slope suggests formation of a complex with stoichiometry 1 : 2 (ligand:calcium), assuming that the ligand is the two-electron reduced quinol form. At the same time, the peak attributed to the parent BQ compound remains unaffected by cation complexation (Fig. 5a, peak I and S2a) confirming that only hydroxylated derivatives are able to form redox sensitive complexes with earth-alkaline metal cations. The structural feature of OHBQ responsible for this property is the presence of at least one pair of adjacent carbonyl-oxygens introduced by a single hydroxide addition to BQ. Compounds 1 and 2 (Fig. 4) on the other hand are capable of binding two Ca^{2+} having two of those pairs.

Biological antioxidants and radical scavengers. The redox potential of OHBQ lowered by 360 mV with respect to the parental compound is indicative for an increased reducing power. Therefore, the radical

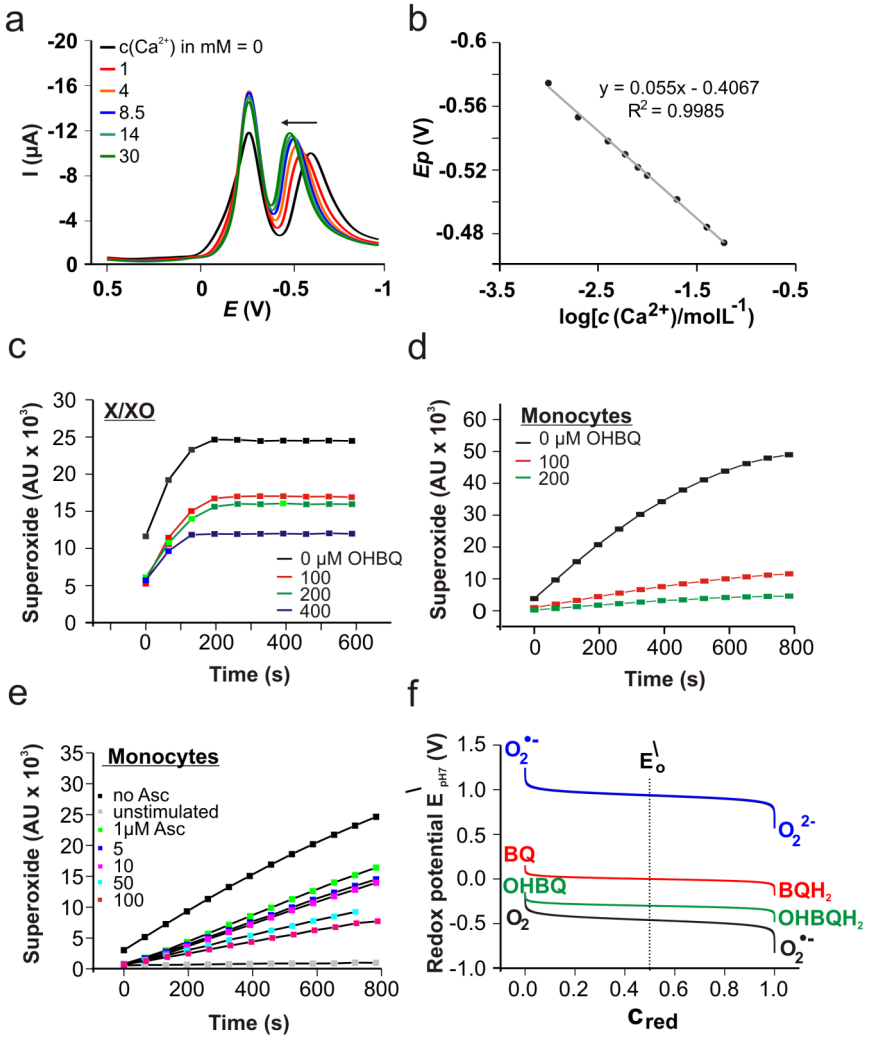

Figure 5 | Ca^{2+}-binding and antioxidant properties of OHBQ derivatives. a) Ca^{2+} sensitivity of the net SW voltammograms of the reaction mixture at pH 7.4, after incubation of 10 µM BQ in NaOH. SW frequency f = 8 Hz, amplitude Esw = 50 mV, and potential step dE = 1 mV. b) Net SWV peak potential dependence on logarithm of Ca^{2+} concentration for the response of OHBQ. Evaluation of the antioxidative properties of OHBQ by ESR spin monitoring using the cyclic hydroxylamine CMH and superoxide ($^{\bullet}O_2^-$) generated by c) xanthine/xanthine oxidase (500 µM/0.05 U/mL) and d) PMA (1 µM) activated primary human monocytes (5×10^5 cells). e) Ascorbic acid as scavenger for monocyte-produced $^{\bullet}O_2^-$ instead of OHBQ (2.5×10^5 cells). f) Comparison of the standard redox potentials at pH 7 of the couples BQ/BQH_2, $OHBQ/OHBQH_2$ with the oxygen redox potentials, calculated as a function of normalized reduced fraction C_{red}.

scavenging and potential antioxidative properties of OHBQ were evaluated by ESR spectroscopy using the xanthine/xanthine oxidase system (Fig. 5a) or stimulated primary human monocytes (Fig. 5d) as a source of $^{\bullet}O_2^-$. In both cases, OHBQ efficiently competes with the spin reagent CMH for $^{\bullet}O_2^-$ indicated by the concentration dependent decrease of the ESR intensity of the CMH radical used as a measure of available superoxide radicals. The $^{\bullet}O_2^-$ scavenging efficiency in the monocyte system is even slightly higher than the effect of equivalent amounts of ascorbic acid (Fig. 5e). Our results indicate that the OHBQs, stabilized in their reduced (quinol) form in aerated solution, are responsible for the distinct antioxidant and superoxide scavenging properties. This particular feature is also reflected by the strong negative value of the reduction potential (Fig. 5f), which represents the formal driving force for the reduction of $^{\bullet}O_2^-$ (electron from $OHBQH_2$ to $^{\bullet}O_2^-$, upper couple). Although BQH_2 has a considerable driving force for reduction of $^{\bullet}O_2^-$, this reduced species is not stable in aerated solutions as seen in Fig. 2a. This highlights the more powerful antioxidative potential of these hydroxylated quinone derivatives.

Discussion

Based on our experimental data, we propose mechanistic pathway(s) for formation of hydroxyl BQ derivatives upon chemical reaction of BQ and NaOH, the first step of which is nucleophilic substitution as proposed in[18] and/or Michael nucleophilic addition of a hydroxyl anion to the BQ quinone form (I) thus yielding mono-hydroxylated BQ forms (Fig. 6a). Compounds II and III in Fig. 6a are most probably present in their di-anionic state (II^{2-} and III^{2-}) in the alkaline environment, and have a reducing potential. Next, by a single electron transfer (SET) to compound I, the primary radical $I^{\bullet}$ is formed which was identified in ESR in alkaline solution (Fig. 3a, b and simulation parameters of hyperfine couplings: six equivalent CH_3-protons 0.795 G, two ring protons: 1.453 G). This primary radical can also transiently be seen upon reduction with $NaBH_4$ in aqueous

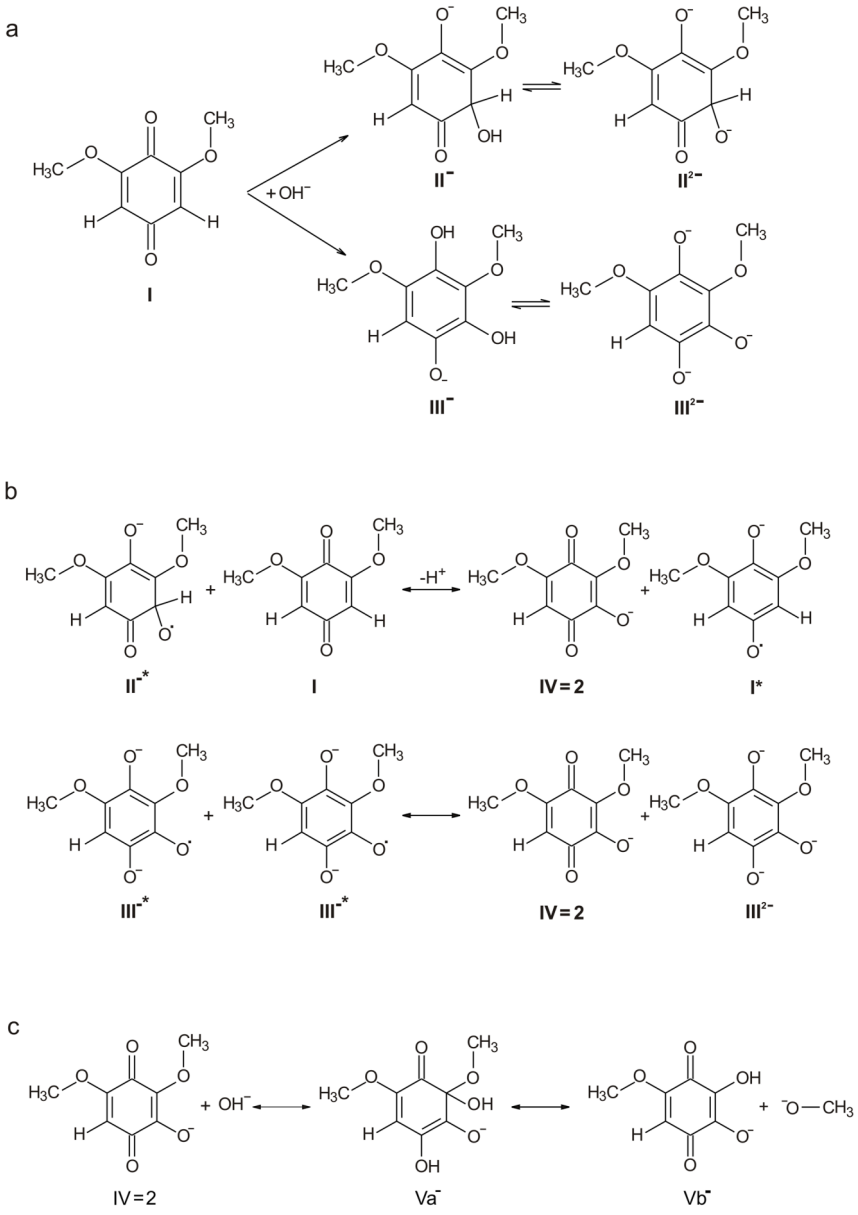

Figure 6 | Chemical transformation of BQ in alkaline environments. a) Formation of reducing species upon hydroxylation of 2,6-dimethoxy benzoquinone (I). b) Possible reactions of formation of the primary radical and a mono-hydroxylated species (IV). c) Formation of the di-hydroxylated species and release of methanol.

neutral solution, but is re-oxidized within around 10 min (not shown). The radicals of II and III, in principle, can transfer a second electron to I, and, via loss of H^+ for II (Fig. 6b), transform to the species IV which is identical to product 2 found with HPLC-MS (Table 1). Additionally, a disproportionation reaction of radical III will also lead to formation of IV (Fig. 6b). In this way, BQ (I) is consumed and transformed via radical I to the mono-hydroxylated form IV. None of the radicals of II and III are sufficiently stable in the alkaline solution to be observed in ESR.

Species IV is not apparent (and stable) as a radical, but is most probably the precursor for the di-hydroxylated forms. The OH^- addition appears more likely to occur at the carbon in position 2 of IV because of its polarization by adjacent electron withdrawing groups, but not at the remaining quinoid ring proton position. As indicated in Fig. 6c, the di-hydroxylated species Vb may be formed via the intermediate Va by liberation of methanol as observed in NMR (Fig. 3). Species Va, possessing reductive properties like compounds II or III, is transformed by SET and loss of methanol to radical $Vb^{\bullet}$. On the other hand, any radical or reducing species present in the alkaline solution can reduce Vb to the semiquinone radical form $Vb^{\bullet}$. This radical is consistent with the EPR parameters for one quinoid proton, one methyl group and a small exchangeable proton with a high pK_a (simulation parameters: C-H, 2.51G; OCH_3, 0.7G; OH, 0.19G). In principle, radical $Va^{\bullet}$ cannot be excluded as a possible origin of this EPR signal, which, however, is then requiring, that one methyl-group is hidden in the spectral line width of less than 0.01 mT. It should be noted, that the radical state $Va^{\bullet}$ can also transform to Vb, when the methoxy group leaves as a radical. This methanol radical could then react with other radicals or even form new radicals. However, no clear indications of a methanol radical were found in our experiments.

The kinetic behavior of the two radicals observed in EPR (Fig. 3a) can be followed over more than 24 h. The formation of the primary radical $I^{\bullet}$ appears to be associated with the first hydroxylation step. Because of the multiple species present, the exact mechanistic details, particularly of its decay remain elusive. The rather persistent secondary radical is obviously formed upon or after the second hydroxylation in considerable amounts. Its kinetic curve is well described by a sequential reaction model (with reaction constants $k_1 = 1 \cdot 10^{-5}\ s^{-1}$ and $k_2 = 1.6 \cdot 10^{-4}\ s^{-1}$). It is also noted that oxygen dissolved in the alkaline solution is not affecting the reaction, because the same radicals and same kinetic behavior was found in anoxic solution prepared in an anaerobic tent (not shown).

Species Vb is not appearing as a major product in the HPLC/DAD/MS-analysis after re-titrating to neutral pH, but it constitutes one part (structures 4 M′ and 5 M′ in Fig. 4) of the higher molecular weight fused ring structures 4 and 5. The other part of compound 4 is a tetra-hydroxylated BQ-species (4 M″ in Fig. 4), which may be produced by further successive OH^- addition to Vb, also possibly involving transient radical species not observed in EPR. In neutral solution, Vb (4 M′) and 4 M″ are combining in a condensation reaction to yield the dimeric compound 4 detected by HPLC/MS. Its one electron reduced form, in principle, could also explain the EPR pattern of the second radical in alkaline medium, provided that the dimer is formed under these conditions. Finally, combination of Vb with the oxidized form of the compound 1 (Table 1), a tri-hydroxylated species arising from a further OH^- addition to Vb, yields the compound 5.

Considering the experimental information accumulated up to now, the reaction pathways forming the major compounds suggested by HPLC/DAD/MS and the radicals detected by ESR are conclusive. More species may exist during the course of reaction as is indicated by the broad peak in UV/VIS spectra and multiple lines in NMR in the region of methoxy signals.

In summary, we have analyzed in detail the spectral and electrochemical behavior of the naturally occurring 2,6-dimethoxy-1,4-benzoquinone and have clarified the reaction mechanisms in which BQ is transformed into novel OHBQ derivatives. The newly identified OHBQ derivatives show that a hydroxyl group can be easily attached to the free position of the quinone ring and, in particular, that at least one methoxy group can be substituted with a hydroxyl group. It is important to note that the chemical approach to produce hydroxylated derivatives chosen here can in principle be replaced by the action of monooxygenases or other hydroxylating enzymes in organisms[19,29,30]. The obtained hydroxylated species are rather stable under physiological conditions and possess a remarkable radical scavenging potential. In addition, they efficiently and selectively form complexes with earth-alkaline metal cations, particularly with the physiologically important Ca^{2+}. Both of these properties should be relevant under *in vivo* conditions. Further studies are needed to fully uncover the potential pharmacological use and the biological importance of naturally occurring or metabolically produced hydroxylated quinones.

Methods

Reagents and Solutions. All the chemicals used were purchased from Sigma-Aldrich (Germany), if not otherwise stated. All solutions were prepared using deionized water (Millipore).

Preparation of hydroxylated derivatives of 2,6-dimethoxy-1,4-benzoquinone. Appropriate amounts of solid 2,6-dimethoxy-1,4- benzoquinone were dissolved into 0.1 to 0.01 mol/L alkaline solution of NaOH. After defined time periods the reaction mixture was quenched by titrating to neutral pH with HCl (5 mol/L).

Electrochemistry. Cyclic voltammetry (CV) and square-wave voltammetric (SWV) electrochemical experiments were performed with a Potentiostat model AUTOLAB PGSTAT12 (Eco Chemie, the Netherlands) in conventional three-electrode set-up. An Ag/AgCl (3 mol/L KCl) was used as a reference electrode, while the Platinum wire served as a counter electrode. The working electrode was a glassy carbon electrode (Metrohm) with diameter of 3 mm. The working electrode was cleaned immediately before each experiment by polishing it with Aluminum powder for 30 s, and rinsing with deionized water. All experiments were performed at room temperature (22 ± 2°C). Metal binding experiments with defined concentrations of OHBQ derivatives were performed in presence of 0.1 – 50 mM chloride salts of Ca^{2+}, Ba^{2+} and Mg^{2+}. Both CV and SWV were used to record the shifts of the peak potential in dependence of the earth-alkaline metal ion concentration in the measuring solution. From the thermodynamic shifting the stoichiometry and the stability constants were derived (see ref. 19 for details).

UV-VIS. For the spectrophotometric experiments a UV/VIS Spectrophotometer Model Ultrospec 2110 pro was used. The measurements covered a spectral range from 200 to 900 nm.

EPR and NMR. The EPR experiments were performed at room temperature with a Bruker spectrometer (ESP300e) equipped with a TMH cavity. The modulation amplitudes varied between 0.001 mT and 0.02 mT depending on the sample. The microwave power was set to 0.2 or 0.63 mW. Spectra were recorded with scan times of 10, 50 or 90 s and stored consecutively to monitor the kinetic behavior of the radicals. The BQ samples were prepared either at pH 13 or 14 in the presence or absence of oxygen (using de-aerated solutions and an anaerobic tent), and were filled into a gastight flat cell (Wilmad). For reduction with sodium borhydride ($NaBH_4$), its concentration was always half of the BQ concentration. The EPR spectra of the BQ reaction were evaluated with the home made program Medeia which measures the peak-to-peak intensity and width of one (or several) lines of a radical visible in a time series. In the absence of line width changes and saturation effects, the intensity information can be translated to radical concentration by calculating the integral of the monitored line and considering the multiplicity of the radical signal. This value is compared to a reference sample of known concentration recorded under identical, non-saturating conditions. The interaction of superoxide radical with the new BQ forms was assessed by EPR measurements of the Xanthine/Xanthine oxidase (X/XO) assay and with stimulated human monocytes as $^{\bullet}O_2^-$ sources. The redox activated cyclic hydroxylamine spin trap CMH (1-hydroxy-3-methoxycarbonyl-2,2,5,5-tetramethylpyrrolidine) was used in 300 μM concentration for all experiments to monitor $^{\bullet}O_2^-$ production. The EPR spectra of the CMH radical were measured with modulation amplitude of 0.1 mT and a microwave power of 20 mW. For the X/XO system 0.05 U/mL of XO, 500 μM xanthine and CMH were mixed in 50 mM Phosphate buffer pH 7.4, and 50 μL were filled in a glass capillary, which was quickly inserted into the capillary holder and kept at 25°C in a temperature controller (BioIII TGC, Noxygen) during the measurement. Monocytes were counted, 250.000 cells were taken for experiments and stimulated with phorbol esther (PMA, 1 μM). CMH was the spin reagent. All experiments were performed with Ringer's buffer at 37°C in 50 μL glass capillaries. The oxygen concentration of all solution was about 200 μM. For both systems, all control experiments with single components of the assays and

CMH were tested for unwanted radical production. In addition, $^{\bullet}O_2^-$ was identified by suppression of the CMH signal by superoxide dismutase SOD (100 U/mL) as superoxide scavenger. For the NMR experiments, a 400 MHz Bruker Avance instrument was used to record standard one-dimensional proton spectra. The solutions were prepared in D2O and titrated to pD 7 with DNO3 after defined reaction times in 1 M or 0.1 M NaOD. The samples (600 μL) were filled in precision quartz tubes for measurement at 290 K. Tetra-methyl-silane (TMS) was used as an internal standard.

HPLC/DAD/ESI-MSn. Chromatographic separations were carried out on 150 mm × 4.6 mm, 5 μm XDB-C18 Eclipse column (Agilent, USA). The mobile phase consisted of two solvents: water-formic acid (1%, V/V) and acetonitrile. A linear gradient was used starting with 30% acetonitrile to reach 100% acetonitrile at 30 min. The flow rate was 0.8 mL min-1, and the injection volume 5 μL. The HPLC system was equipped with an Agilent 1100 series diode array detector (DAD) coupled to a mass spectrometer (Agilent Technologies, Waldbronn, Germany). It consisted of a G1312A binary pump, a G1313A autosampler, a G1322A degasser and G1315B photo-diode array detector, controlled by ChemStation software (Agilent, v.08.03). Spectral data from all peaks were accumulated at 190–600 nm and chromatograms were recorded at 280 nm. The mass detector was a G2445A Ion-Trap Mass Spectrometer equipped with an electrospray ionisation (ESI) system and controlled by LCMSD software (Agilent, v.6.1.). Nitrogen was used as nebulizing gas at pressure of 65 psi and the flow was adjusted to 12 L min-1. The heated capillary temperature was 325°C and the voltage was 4 kV. MS data were acquired in the positive ionization mode. The full scan mass covered the m/z range from 15–500. Collision–induced fragmentation experiments were performed in the ion trap using helium as a collision gas, with voltage ramping cycle from 0.3 up to 2 V. The maximum accumulation time of the ion trap and the number of MS repetitions to obtain the MS average spectra were set at 300 ms and 3, respectively.

Isolation and cultivation of primary human monocytes. Research carried out for this study with human material has been approved by the local ethics committee. Primary human monocytes were isolated from peripheric blood leucocytes (PBLs). PBLs were obtained from leucocyte-reducing-system chambers (kindly provided by the Department of Haemostaseology, UKS). The cells were separated from the rest of blood content by a Ficoll density gradient centrifugation. Remaining erythrocytes and thrombocytes were abolished by erythrocyte lysis (using buffer containing NH_4Cl, $KHCO_3$ and EDTA) and gentle centrifugation. Monocytes were isolated from PBLs (in PBS + 0.5% BSA) either by negative isolation or by adhesion. Negative isolation was performed using the Dynabeads® Untouched™ Human Monocytes System (Invitrogen, 113.50D) following the manufacturer instructions. For isolation by adhesion, PBLs were transferred into standard culture flasks containing 30 ml RPMI media (10% FCS, 0.1% Penicillin/Streptomycin, 37°C/5% CO_2) for 2 h, followed by growth media exchange and additional 24 h of incubation. Cells were washed with PBS (containing 0.5% BSA), scratched from the surface and suspended into RPMI containing 10% FCS, without antibiotics. After isolation, cells were cultured in RPMI (10% FCS) in 24-Well Plates (Ultra-Low Attachment Surface, Corning Incorporated, 3473), with a density of $1-4 \times 10^6$ cells/ml. Purification and cell quality was determined by FACS (CD14, CD11c expression and IgG2a isotype binding) and immunohistochemistry (CD14 expression) revealing a purity of > 90%.

1. Lester, R. L., Crane, F. L. & Hatefi, Y. Coenzyme Q - a New Group of Quinones. *J. Am. Chem. Soc.* **80**, 4751–4752 (1958).
2. Lester, R. L. & Crane, F. L. Natural Occurrence of Coenzyme-Q and Related Compounds. *J. Biol. Chem.* **234**, 2169–2175 (1959).
3. Crane, F. L. Biochemical Functions of Coenzyme Q10. *J. Am. Coll. Nutr.* **20**, 591–598 (2001).
4. Turunen, M., Olsson, J. & Dallner, G. Metabolism and function of coenzyme Q. *Bba-Biomembranes* **1660**, 171–199 (2004).
5. Powis, G. Free radical formation by antitumor quinones. *Free Radical Biology and Medicine* **6**, 63–101 (1989).
6. Lown, J. W. The mechanism of action of quinone antibiotics. *Molecular and Cellular Biochemistry* **55**, 17–40 (1983).
7. Bentinger, M., Brismar, K. & Dallner, G. The antioxidant role of coenzyme Q. *Mitochondrion* **7**, S41–S50 (2007).
8. James, A. M., Smith, R. A. J. & Murphy, M. P. Antioxidant and prooxidant properties of mitochondrial Coenzyme Q. *Arch. Biochem. Biophys.* **423**, 47–56 (2004).
9. Bartlet, P. N. Bioelectrochemistry; fundamentals, experimental techniques, and applications. (Wiley, 2008).
10. Gordillo, G. J. & Schiffrin, D. J. The electrochemistry of ubiquinone-10 in a phospholipid model membrane. *Faraday Discuss.*, 89–107; discussion 171–90 (2000).
11. Rich, P. R. Electron transfer reactions between quinols and quinones in aqueous and aprotic media. *Bba-Bioenergetics* **637**, 28–33 (1981).
12. Quan, M., Sanchez, D., Wasylkiw, M. F. & Smith, D. K. Voltammetry of quinones in unbuffered aqueous solution: reassessing the roles of proton transfer and hydrogen bonding in the aqueous electrochemistry of quinones. *J. Am. Chem. Soc.* **129**, 12847–56 (2007).
13. Manojkumar, T. K., Choi, H. S., Tarakeshwar, P. & Kim, K. S. Ab initio studies of neutral and anionic p-benzoquinone--water clusters. *The Journal of Chemical Physics* **118**, 8681–8686 (2003).
14. Bolton, J. L., Trush, M. A., Penning, T. M., Dryhurst, G. & Monks, T. J. Role of Quinones in Toxicology†. *Chemical Research in Toxicology* **13**, 135–160 (2000).
15. Nohl, H., Jordan, W. & Youngman, R. J. Quinones in Biology: Functions in electron transfer and oxygen activation. *Advances in Free Radical Biology & Medicine* **2**, 211–279 (1986).
16. Swenton, J. Chemistry of Quinones (John Wiley, New York, 1988).
17. Brunmark, A. & Cadenas, E. Redox and addition chemistry of quinoid compounds and its biological implications. *Free Radical Biology and Medicine* **7**, 435–477 (1989).
18. Pedersen, J. A. On the application of electron paramagnetic resonance in the study of naturally occurring quinones and quinols. *Spectrochim. Acta A Mol. Biomol. Spectrosc.* **58**, 1257–70 (2002).
19. Bogeski, I. *et al.* Calcium binding and transport by coenzyme Q. *J. Am. Chem. Soc.* **133**, 9293–303 (2011).
20. Cosgrove, D. J. *et al.* Isolation of methoxy- and 2:6-dimethoxy-p-benzoquinone from fermented wheat germ. *Nature* **169**, 966–7 (1952).
21. Tran, U. C. & Clarke, C. F. Endogenous synthesis of coenzyme Q in eukaryotes. *Mitochondrion The Role of Coenzyme Q in Cellular Metabolism: Current Biological and Clinical Aspects* **7**, S62–S71 (2007).
22. Baxendale, J. H. & Hardy, H. R. The ionization constants of some hydroquinones. *Transactions of the Faraday Society* **49**, 1140–1144 (1953).
23. Bishop, C. A. & Tong, L. K. J. Equilibria of substituted semiquinones at high pH. *Journal of the American Chemical Society* **87**, 501–505 (1965).
24. Holton, D. M. & Murphy, D. The electron spin resonance spectra of semiquinones obtained from some naturally occurring methoxybenzoquinones. *Journal of the Chemical Society, Perkin Transactions* **2**, 1757–1759 (1980).
25. Ashworth, P. & Dixon, W. T. Secondary radicals in the autoxidation of hydroquinones and quinones. *J. Chem. Soc. Perk. T.* **2**, 1130–1133 (1972).
26. Pedersen, J. A. Electron spin resonance studies of oxidative processes of quinones and hydroquinones in alkaline solution; formation of primary and secondary semiquinone radicals. *J. Chem. Soc. Perk. T.* **2**, 424–431 (1973).
27. Bennett, I. M. *et al.* Active transport of Ca2+ by an artificial photosynthetic membrane. *Nature* **420**, 398–401 (2002).
28. Mirceski, V., Gulaboski, R., Bogeski, I. & Hoth, M. Redox Chemistry of Ca-Transporter 2-Palmitoylhydroquinone in an Artificial Thin Organic Film Membrane. *J. Phys. Chem. C* **111**, 6068–6076 (2007).
29. Bernhardt, R. Cytochromes P450 as versatile biocatalysts. *J. Biotechnol.BioPerspectives--From basic research to industrial production* **124**, 128–145 (2006).
30. Sono, M., Roach, M. P., Coulter, E. D. & Dawson, J. H. Heme-Containing Oxygenases. *Chem. Rev.* **96**, 2841–2888 (1996).

Acknowledgements

We are very grateful to Drs. B. Morgenstern and B. Kutzky for their help with the NMR experiments. RG acknowledges the "AvH" foundation for providing a Return Fellowship. This project was funded by the DFG (SFB 894 and GK845, to MH, BO 3643/2-1 and SFB 1027 to IB and RK 1242/1-1 to RK) and Saarland University (HOMFOR Excellent to IB). This work is also supported by the AvH foundation via the joint German-Macedonian project, 3.4-Fokoop-DEU/1128670 (to VM, RG, IB and MH).

Author contributions

Designed research: R.G., I.B., R.K., V.M., M.H.; Performed research: R.G., I.B., R.K., S.S., B.P., H.H.H., J.P.S., M.S.; Analyzed data: R.G., I.B., R.K., S.S., V.M., H.H.H., J.P.S., M.S.; Wrote the paper: R.G., I.B., R.K., V.M., M.H.

Additional information

Supplementary information accompanies this paper at http://www.nature.com/scientificreports

Competing financial interests: R.G., I.B., R.K. and M.H. declare that some of the results presented in this MS are part of the European patent "Benzoquinone based antioxidants" Patent No. 09178735.8-2103, European Patent Office, Munich, Germany. The other authors have no competing financial interests.

How to cite this article: Gulaboski, R. *et al.* Hydroxylated derivatives of dimethoxy-1,4-benzoquinone as redox switchable earth-alkaline metal ligands and radical scavengers. *Sci. Rep.* **3**, 1865; DOI:10.1038/srep01865 (2013).